

Electrical Transport in Terbium-iron-transition Metal Mixed Oxides

U.P. SINGH, A.N. THAKUR*, S.V. SINGH and S.C. KUMAR
Department of Physics, T.D. Postgraduate College, Jaunpur-222 002, India

This paper presents the results of electrical conductivity (σ) and seebeck coefficient (S) measurements on the pressed pellets of TbFeTO₄ (where T = Fe, Cr, Mn and Co) in the temperature range 400-1200 K. It has been found that these compounds are essentially electronic semiconductor with σ values lying in the range 10^{-7} to $10^{-3}\Omega^{-1} \text{ m}^{-1}$ around 408 K. The maximum value of σ has been observed for TbFeMnO₄ and lowest for TbFe₂O₄. The log σT vs. T^{-1} as well as S vs. T^{-1} plots for the studied compounds have three linear regions separated by break temperatures T_1 and T_2 which are same in both the plots. The sign of S indicates that charge carriers are electrons in the studied temperature range. The electrical conduction in first range ($T < T_1$) is extrinsic and occurs due to donor type centers. In the second ($T_1 < T < T_2$) and third ($T > T_2$) ranges, electrical conduction is hopping type and occurs due to hopping of electrons from Fe²⁺ to Fe³⁺ in TbFe₂O₄, Co²⁺ to Fe³⁺ in TbFeCoO₄ and Fe²⁺ to Cr³⁺ in TbFeCrO₄. In TbFeMnO₄, electrical conduction occurs due to hopping of electrons from Mn³⁺ to Mn⁴⁺ centers in the temperature range $T_1 < T < T_2$ and from Fe²⁺ to Mn³⁺ centers in the range $T > T_2$.

Key Words: Electrical conductivity, Seebeck coefficient, Terbium-iron-transition metal mixed oxides.

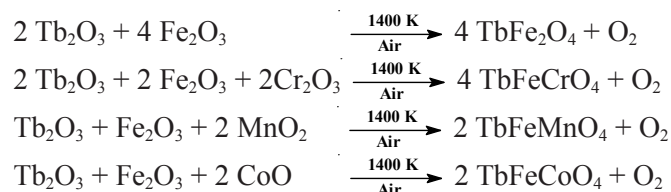
INTRODUCTION

Mixed rare-earth and transition metal oxides have been the subject of study due to their interesting magnetic, dielectric, electrical transport properties and their applications¹⁻³. Several such materials have been investigated in the past⁴⁻⁹. The 3 *d* elements in many of these mixed compounds have variable valence state and yield interesting magnetic, dielectric and electrical transport properties. Expecting some interesting results, we have prepared and studied rare-earth-iron-transition metal mixed oxides. Some of these studies have been reported by us earlier^{10,11} and one of the similar studies on terbium-iron-transition metal mixed is reported in this paper. The literature survey showed that only limited studies are reported on the compounds of this series. The only studied materials in the entire series are

YFe₂O₄, GdFe₂O₄ and LuFe₂O₄. These studies are related with their preparation and low temperature phase transition^{12,13}, neutron diffraction and magnetic properties^{14,15}, dielectric study¹⁶ and Mossbauer data^{17,18} and low temperature electrical transport have been explained¹⁹. No high temperature electrical transport study on the materials of this series is reported in literature. It has been reported that qualitative understanding and semi-qualitative analysis of the conduction mechanism can be presented by studying the electrical conductivity and Seebeck coefficient as a function of various parameters²⁰⁻²². Using same methodology, we have investigated the electrical transport mechanism of terbium-iron-transition metal mixed oxides and results are presented in this paper.

EXPERIMENTAL

The starting materials for the preparation of these compounds were Tb₂O₃ (99.99 % purity from Johnson Chemical Company, India), Fe₂O₃ (99.99 % purity from Riedal Danaen AG, Seeize Hannover, Germany) and oxides Cr₂O₃, CoO and MnO₂ (99.99 % purity from Rare and Research Chemical, Mumbai, India). These starting materials were first heated around 400 K for 5-6 h before use. The stoichiometric amount of these oxides were mixed and heated in silica crucible for 50 h at a temperature of 1400 K. In this process mixture was followed by one intermediate grinding and final product was cooled down slowly. The starting materials undergo following solid state reaction and yield desired compounds.



The weight loss corresponding to oxygen on the right hand side of the reactions were observed in all cases except in TbFeMnO₄. In this case, the loss was less than expected. The details are described elsewhere²³.

To get the confirmation regarding the complete formation of the prepared compound, X-ray diffraction study have been carried out at room temperature using CuK_α radiation (λ = 0.15418 nm). From X-ray diffraction pattern d_{hkl} have been evaluated using relation

$$d_{\text{hkl}} = \frac{0.145418 \times 10^{-9}}{2 \sin \theta} \quad (1)$$

from the values of d_{hkl}, structures of the studied compounds were resolved using usual procedure. All peaks have been identified and assigned proper hkl values. This confirmed that the prepared compounds are in single phase.

The measurements of electrical conductivity (σ) and Seebeck coefficient (S) were performed on pressed pellets because of difficulties in growing large single crystal of these compounds needed for such measurements due to their high melting point and our limited facilities. The details of these measurements including electrode preparation, *etc.* are given elsewhere^{6,23}.

RESULTS AND DISCUSSION

The analysis of XRD data shows that all compounds have orthorhombic unit cell with cell parameter as given in Table-1.

TABLE-1
STRUCTURAL PARAMETERS OF ORTHORHOMBIC UNIT CELL,
CALCULATED DENSITY, DENSITY OF PREPARED PELLETS AND
VALUES OF PORE FRACTION

| Compound | Lattice parameter (nm) | | | Density $\text{K g}^{-3} \times 10^{-3}$ | | |
|----------------------------------|------------------------|--------|--------|--|--------------------------|-------------------|
| | a_0 | b_0 | c_0 | Calcd. (d_o) | Pressed pellet (d_p) | Pore fraction (f) |
| TbFe ₂ O ₄ | 0.6246 | 0.7366 | 0.8836 | 5.34 | 4.69 | 1.118 |
| TbFeCrO ₄ | 0.6340 | 0.7482 | 0.8850 | 5.14 | 4.30 | 0.163 |
| TbFeMnO ₄ | 0.6174 | 0.7286 | 0.8850 | 5.05 | 4.28 | 0.153 |
| TbFeCoO ₄ | 0.6280 | 0.7410 | 0.8915 | 5.20 | 4.50 | 0.153 |

In order to evaluate bulk value of electrical conductivity and Seebeck coefficient of crystalline solid, the study of pellets density, electrical conductivity and Seebeck coefficients have been done as a function of pelletizing pressure²³. It has been found that density of pressed pellets (d_p) depends upon pelletizing pressure (P). In all cases, density of pellets increase linearly with P upto a value of $P = 5.28 \times 10^8 \text{ Nm}^{-2}$, then the increase becomes slow and it becomes almost constant for $P \geq 6.32 \times 10^8 \text{ Nm}^{-2}$. The maximum density of highest pressed pellet (d_p) remains less than calculated density (d_o). The difference obviously occurs due to pore fraction (f) which have been determined by the relation.

$$f = \frac{d_o - d_p}{d_o} \quad (2)$$

The values of d_o , d_p and f for the studied materials are given in Table-1. It is seen from this table that the pore fractions are small enough to evaluate any bulk parameter by suitable correction. The electrical conductivity of several pellets (σ_p) of each compound made at different P has been measured using similar electrode at a fixed temperature. The log σ_p vs. P plot for each compound shows that it increases with P and tends to become

constant for P exceeding $6.32 \times 10^8 \text{ Nm}^{-2}$. This constancy of σ_p with P ensures significant reduction of grain boundaries but $d_p < d_o$ indicates that crystalline value of σ may be significantly more than σ_p . The estimation of σ from maximum value of σ_p has been done using relation^{7,24}.

$$\sigma = \sigma_p \left\{ 1 + \frac{f}{1 + f^{2/3}} \right\} \quad (3)$$

Seebeck coefficient (S) has also been measured for number of pellets of each compound made at P ranging from 3.12×10^8 to $8.4 \times 10^8 \text{ Nm}^{-2}$. Within our experimental accuracy, we do not observe any dependence of S on P . Hence S needs no correction for crystalline solid. This is logically expected because S measurement involves measurement of voltage across the sample pellet when current flow is zero, hence pore fraction does not come in the picture.

Electrode plays an important role in the measurement of σ . For such measurement ohmic contact between the pellet and electrode interface is essential²⁴. Even in the case of ohmic contact, we have measured current through the pellet at different applied voltage at constant temperature. Using dimension of the pellet current density (J) and electric field (E) have been evaluated. It has been found that for pellet of studied materials, J vs. E plots are straight line upto $E \sim 6.0 \times 10^3 \text{ v/m}$, ensuring ohmic contact between pellet and electrode interface.

Since several superfluous effects not connected with bulk property of the material can arise due to grain boundaries, it is essential to see that grain boundary effects have been minimized in highly pressed pellets by using very fine grain powders. This can be checked by measuring σ at different AC signal frequencies. Here, σ_p has been measured at AC, 100 Hz, 1 and 10 KHz and a plot of $\log \sigma_p$ vs. $\log f$ has been obtained. It has been observed that $\log \sigma_p$ is independent for $\log f$. The DC and AC values of σ_p have been found to be same. This indicates that grain boundary effects are considerably minimized in highly pressed pellets.

The DC current density through the pellet of all studied materials has been measured as a function of time at constant temperature and applied DC field. It is found that J is independent of time. This observation indicates that the electrical conductivity of studied compounds is essentially electronic and ionic conductivity is negligibly small.

The electrical conductivity (σ) measurement of few pellets of each studied material has been carried out in the temperature range 400 to 1200 K. The measurements have been done on pellets made at $P > 6.32 \times 10^8 \text{ Nm}^{-2}$ and sintered around 1000 K for 50 h. The σ_p values do not differ for different samples and are also independent of pellet dimensions. Further, no difference in σ_p values has been found during heating and cooling cycles.

It also remains almost same irrespective of thermal history and self life of the pellet. The mean value of σ_p for few pellets of each compound has been taken as the bulk value of σ_p . The σ values have been evaluate using eqn. 3. The plots of $\log \sigma T$ vs. T^{-1} for different studied materials are shown in Fig. 1. It is seen from these figures that each plot can be divided into three liner regions namely range I for $T < T_1$, range II for $T_1 < T < T_2$ and range III $T > T_2$. T_1 and T_2 have been termed as break temperatures. In each region, the variation of $\log \sigma T$ vs. T^{-1} can be represented by the relation.

$$\sigma T = \sigma_{\sigma T} \exp(-E_a/kT) \quad (4)$$

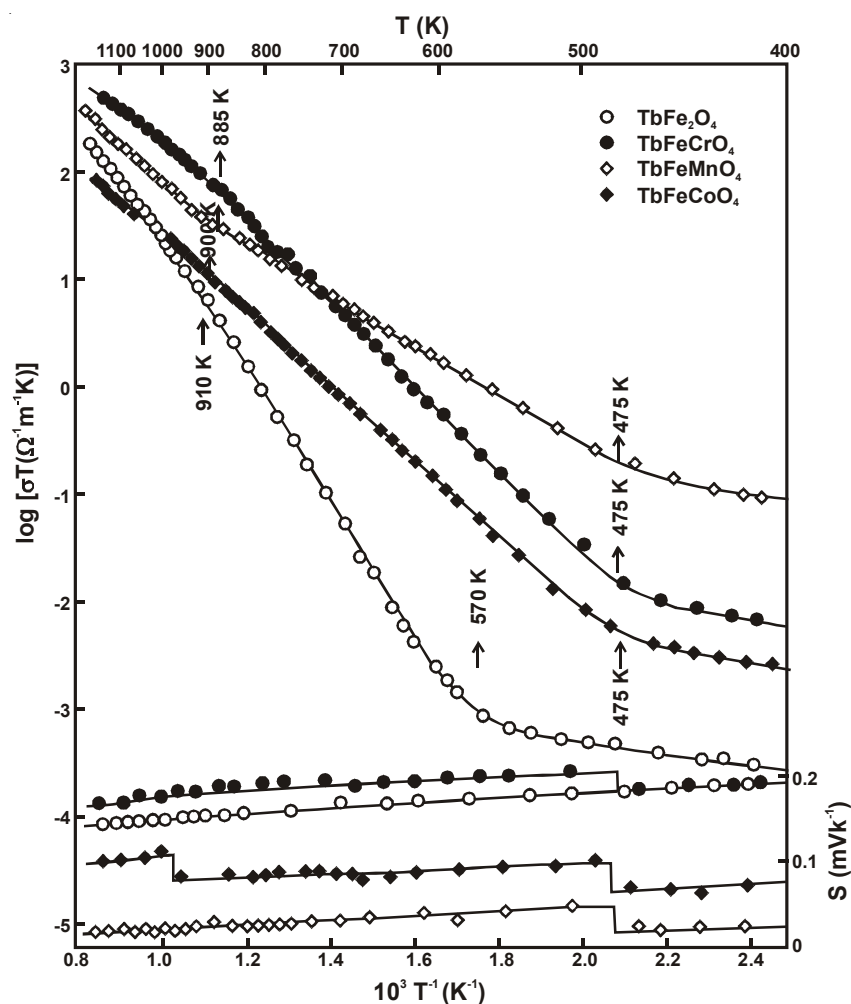


Fig. 1. Plots of logarithmic of product of electrical conductivity and temperature ($\log \sigma T$) and Seebeck coefficient (S) against inverse of absolute temperature ($10^3/T$) for TbFe_2O_4 , TbFeCoO_4 , TbFeCrO_4 , TbFeMnO_4

The values of pre-exponential constant (σ_{0T}) and activation energy (E_a) have been evaluated from the experimental plot and are given in Table-2 together with the values of T_1 and T_2 .

TABLE-2
VALUES OF PRE-EXPONENTIAL CONSTANT (σ_{0T}) AND E_a
TOGETHER WITH T_1 AND T_2 IN DIFFERENT REGIONS OF
 $\log \sigma T$ vs. T^{-1} PLOT OF THE STUDIED MATERIALS

| Compound | $T < T_1$ | | | $T_1 < T < T_2$ | | | $T > T_2$ | |
|----------------------------------|---|---------------|--------------|---|---------------|--------------|---|---------------|
| | σ_{0T} ($\Omega^{-1}mK^{-1}$) | E_a (eV) | T_1 (K) | σ_{0T} ($\Omega^{-1}mK^{-1}$) | E_a (eV) | T_2 (K) | σ_{0T} ($\Omega^{-1}mK^{-1}$) | E_a (eV) |
| TbFe ₂ O ₄ | 1.43×10^{-2} | 0.14 | 570 | 8.76×10^7 | 1.28 | 910 | 4.52×10^6 | 1.04 |
| TbFeCrO ₄ | 3.28×10^{-1} | 0.12 | 475 | 1.05×10^4 | 0.74 | 885 | 1.28×10^5 | 0.64 |
| TbFeMnO ₄ | 3.07×10^0 | 0.12 | 475 | 2.25×10^4 | 0.50 | 885 | 6.65×10^5 | 0.72 |
| TbFeCoO ₄ | 6.91×10^{-2} | 0.12 | 475 | 9.67×10^5 | 0.80 | 900 | 1.32×10^5 | 0.64 |

The Seebeck coefficient measurements on different pellets of each compound have also been done. These values do not differ from sample to sample and are also independent of pellet dimension within experimental accuracy which is *ca.* $\pm 10\%$ around 800 K and become *ca.* $\pm 5\%$ around 1000 K. These are nearly same in heating and cooling cycles. The repeated values of S has been recorded for each materials in the temperature range 400 to 1200 K and have been presented in Fig. 1 as S vs. T^{-1} plot. We must point out at this stage that standard convention for the values of S has been used. In this convention, $S = \Delta E/\Delta T$ and has positive sign for negative charge carrier and *vice-versa*. It is observed for S vs. T^{-1} plot that S values are positive throughout the studied temperature range indicating dominance of negative charge carrier in the conduction. S vs. T^{-1} plots can be divided into three linear regions namely range I for $T < T_1$, range II for $T_1 < T < T_2$ and range III for $T > T_2$. T_1 and T_2 have been termed as break temperatures. In each range, plot of S vs. T^{-1} can be represented by the relation.

$$S = \frac{\eta}{eT} + H \quad (5)$$

where η and H are constants for each region. The value of η , H , T_1 and T_2 are given in Table-3.

It has been found that σ_{DC} is independent of time even at relatively higher temperature and for sufficiently long time. Further, no significant difference has been found in σ_{AC} and σ_{DC} values. Also σ_{AC} has been found independent of AC signal frequencies. All these studies indicate that studied materials are essentially electronic conductors and ionic conductivity if any, is significantly small. The Seebeck coefficient has been found

positive throughout the studied temperature range. Hence, electrons are the primary charge carriers in these materials. Around 408 K σ of studied compounds lies in the range 10^{-7} to $10^{-2}\Omega^{-1}\text{m}^{-1}$ and increases with increase of temperature. Thus studied materials are typical semiconductor. The log σT vs. T^{-1} as well as S vs. T^{-1} plots have three linear regions separated by break temperatures T_1 and T_2 . The temperature T_1 and T_2 have been found to be nearly same in σ as well as S plots. No phase change have been found in the studied temperature range. Hence, these break temperatures indicate the change in conduction mechanism in these solids. The values of E_a (*ca.* 0.1 eV) in first temperature range ($T < T_1$) are small for all studied compounds. The pre-exponential constant (σ_{0T}) for all the studied compounds in this temperature range is also small (*ca.* $10^{-1}\Omega^{-1}\text{m}^{-1}\text{K}$). Both these values are not appropriate for intrinsic conduction. Thus we conclude that for $T < T_1$, the electrical conduction in these materials are extrinsic and is due to impurities or defects. However at $T > T_1$, E_a as well as σ_{0T} values are large indicating intrinsic conduction.

TABLE-3
CONSTANT η AND H FOR DIFFERENT REGIONS TOGETHER WITH THE VALUES OF T_1 AND T_2 FOR DIFFERENT STUDIED MATERIALS

| Compound | $T < T_1$ | | | $T_1 < T < T_2$ | | | $T > T_2$ | |
|----------------------------------|----------------|-----------------------------|--------------|-----------------|-----------------------------|--------------|----------------|-----------------------------|
| | η (eV) | H (mVK ⁻¹) | T_1 (K) | η (eV) | H (mVK ⁻¹) | T_2 (K) | η (eV) | H (mVK ⁻¹) |
| TbFe ₂ O ₄ | 0.025 | 0.132 | 570 | 0.031 | 0.121 | 910 | 0.050 | 0.099 |
| TbFeCrO ₄ | 0.037 | 0.085 | 475 | 0.021 | 0.140 | 885 | 0.050 | 0.105 |
| TbFeMnO ₄ | 0.025 | -0.035 | 475 | 0.025 | -0.005 | 885 | 0.026 | -0.007 |
| TbFeCoO ₄ | 0.050 | -0.039 | 475 | 0.025 | 0.053 | 900 | 0.063 | 0.045 |

For $T < T_1$ the electrical conduction is extrinsic and thus in order to explain it, one has to look for possible defects and impurities. A chemical impurity of the order of $\pm 0.1\%$ is expected in these compounds. This has been obtained from the stated purity of the materials used for the preparation of these compounds. In order to explain the conduction mechanism, the appropriate plots are log σ vs. T^{-1} and S vs. T^{-1} . For donor type impurity centers, band conduction yields a conductivity expressed as $\sigma = \sigma_0 \exp(-E_d/kT)$, where E_d is donor ionization energy. For this type of conduction the slope of S vs. T^{-1} and log σ vs. T^{-1} plots should be same²². The slope of log σ vs. T^{-1} can be obtained from the slope of log σT vs. T^{-1} plot. However we have obtained these slopes (E_d) by drawing log σ vs. T^{-1} plot (not shown in the paper). These are given in Table-4.

TABLE-4
VALUES OF E_a , E_d AND η FOR THE STUDIED COMPOUNDS

| Compounds | E_a (eV) | E_d (eV) | η (eV) |
|----------------------------------|------------|------------|-------------|
| TbFe ₂ O ₄ | 0.14 | 0.05 | 0.025 |
| TbFeCrO ₄ | 0.12 | 0.05 | 0.037 |
| TbFeMnO ₄ | 0.12 | 0.10 | 0.025 |
| TbFeCoO ₄ | 0.12 | 0.05 | 0.050 |

It is seen from the Table-4 that η and E_d have nearly same values for all except TbFeMnO₄. This indicates that extrinsic conduction in all other compounds is due to donor type impurities. No exact reason can be given for extrinsic conduction in TbFeMnO₄. However it may be remarked that in the preparation of TbFeMnO₄, the observed oxygen loss is less than expected. Thus some excess oxygen is left in the sample. This oxygen converts itself into O²⁻ ion by taking an electron each from Mn³⁺ center and converting two of them in Mn⁴⁺ center. The distance between the oxygen ion and Mn³⁺ center for this process should be small. With this configuration natural hopping of electron from O²⁻ to Mn⁴⁺ center is expected with lower activation energy. The $E_a = 0.12$ eV is probably due to this process. The process appears more probable in view of the fact that observed electrical conductivity for the compound is highest amongst the studied compounds and slope of S vs. $T^{-1}(\eta \sim 0.025)$ plot is small.

In intrinsic range, the majority charge carriers are electrons as indicated by positive value of Seebeck coefficient. TbFe₂O₄ is an ionic compound as has been concluded by us on the basis of magnetic susceptibility studies²³. Thus, the material will contain Tb³⁺, Fe²⁺ and Fe³⁺ ions. Fe is multivalent and it is natural to think that conduction in this compound occurs *via* hopping of electrons localized on Fe²⁺ to Fe³⁺ sites. The hopping of electrons in LuFe₂O₄ has already been observed through Mossbauer studies^{16,17} and data of σ and S have been explained using this mechanism¹⁸.

The activation energy for hopping is 1.28 eV. The Seebeck coefficient in hopping motion is given by the expression²⁵.

$$S = \frac{k}{e} \left[\frac{S_R^*}{k} - \log_e \left\{ \frac{c}{1-c} \right\} \right] \quad (6)$$

where S_R^* is the effective entropy of the lattice which is temperature independent and $c = n/N$, where n and N are the densities of defects and normal sites respectively. In TbFe₂O₄, $n = N/2$ giving $c = 1/2$ and logarithmic term of S to be zero. Hence,

$$S = \frac{S_R^*}{e} \quad (7)$$

thus S should be temperature independent. Experimental values of S has been found small and nearly temperature independent which supports hopping mechanism.

TbFeCrO₄ is also ionic with Tb³⁺, Fe²⁺ and Cr³⁺ as its constituent ions as concluded by our magnetic susceptibility study²³. The hopping conduction in this compound will occur due to hopping of electrons from Fe²⁺ to Cr³⁺ sites. The activation energy is 0.74 eV.

In TbFeCoO₄, ions are Tb³⁺, Fe³⁺ and Co²⁺ as concluded by our susceptibility studies. The hopping conduction will occur due to hopping of electrons from Co²⁺ to Fe³⁺ centers. The activation energy is 0.80 eV. S has also been found nearly temperature independent as expected.

In all the three compounds the drop in slope of $\log \sigma T$ vs. T^{-1} plot above T_2 is due to smoothing of potential barrier or thermal fluctuations as observed in other compounds²⁵.

In case of YFeMnO₄ the expected ions are Tb³⁺, Fe²⁺ and Mn³⁺. The seebeck coefficient (S) is constant with temperature and positive. Hence the normal conduction should hopping of electrons from Fe²⁺ to Mn³⁺. But the activation energy (E_a) in this compound is small 0.72. Further for $T > T_2$, E_a goes up against the lowering in other compounds. Thus in this temperature range the hopping mechanism appears to be due to different centers. In this regard, it is to be noted that the starting material for the preparation of this compound is MnO₂. Thus Mn³⁺ centers can be found only when excess oxygen is librated in the formation of the compounds. But it has not been found true experimentally. Thus existence of both Mn³⁺ and Mn⁴⁺ centers are expected in this compound together with the excess of oxygen. The value of electrical conductivity of this compound has been found higher in studied series. The extra defects are responsible for higher conductivity. For the temperature range $T_1 < T < T_2$, the conduction mechanism is due to hopping of electrons from Mn³⁺ to Mn⁴⁺. At much higher temperature the hopping of electrons from Fe²⁺ to Mn³⁺ centers takes over the conduction mechanism. The activation energy in the latter case is larger than former.

ACKNOWLEDGEMENTS

One of the authors (ANT) is thankful to the UGC, India for financial assistance.

REFERENCES

1. K.T. Standley, Oxide Magnetic Materials, Oxford, Clayender (1972).
2. E.P. Wohlfarth, A Hand Book of Magnetically Ordered Materials, Amsterdam: North Holland, Vol. 1 and 2 (1980).
3. E.P. Wohlfarth, A Handbook of the Properties of magnetically Ordered Substances, Ferromagnetic Materials, Amsterdam: North Holland, Vol. 3 (1982).
4. V.R. Yadav and H.B. Lal, *Can. J. Phys.*, **57**, 1204 (1979).
5. V.R. Yadav and H.B. Lal, *Japan J. Appl. Phys.*, **18**, 2229 (1979).
6. A.K. Tripathi and H.B. Lal, *Mater. Res. Bull.*, **15**, 233 (1980).
7. A.K. Tripathi and H.B. Lal, *J. Mater. Sci.*, **17**, 1595 (1982).
8. K. Gaur and H.B. Lal, *J. Mater. Sci.*, **19**, 3325 (1984).
9. K. Gaur and H.B. Lal, *J. Mater. Sci.*, **20**, 3167 (1985).
10. A.N. Thakur, K. Gaur and H.B. Lal, *Indian J. Phys.*, **70A**, 225 (1996).
11. A.N. Thakur, K. Gaur, M.A. Khan and H.B. Lal, *Indian J. Phys.*, **71A**, 209 (1997).
12. Y. Nakagawa, M. Imazumi, N. Kimizuka and K. Siratori, *J. Phys. Soc. (Japan)*, **47**, 1369 (1979).
13. M. Tanaka, K. Siratori and N. Kimizuka, *J. Phys. Soc. (Japan)*, **53**, 760 (1984).
14. S. Funasaki, Y. Morii and H.R. Child, *J. Appl. Phys.*, **6**, 4114 (1987).
15. Y. Nakagawa, F. Kawaguchi, T. Hayakawa, Y. Ito, H. Yameda, M. Yoshida, F. Fujii, H. Takaguchi and Y. Tsukuda, *J. Appl. Phys. (Japan)*, **27**, 1572 (1988).
16. A.N. Thakur, K. Gaur and H.B. Lal, *J. Mater. Sci. Lett.*, **11**, 496 (1992).
17. M. Tanaka, J.A. Kimitsu, N. Kimizuka, I. Sindo and K. Siratori, Proc. Int. Conf. Ferrites, Kyoto, p. 119 (1980).
18. M. Imazumi, Y. Nakagawa, M. Tanaka, N. Kimizuka and K. Siratori, *J. Phys. Soc. (Japan)*, **50**, 438 (1981).
19. A. Enomura, S. Asai, Y. Ishiwata, T. Inabe, Y. Sakai, N. Tsuda, M. Tanaka and K. Sirayori, *J. Phys. Soc. (Japan)*, **52**, 4286 (1983).
20. H.B. Lal and K. Gaur, Proc. IV. Int. Workshop on Phys. Dev. Madras, p. 93 (1987).
21. K. Gaur and H.B. Lal, Proc. IV. Int. Workshop on Phys. Dev. Madras, p. 100 (1987).
22. H.B. Lal and K. Gaur, *J. Mater. Sci.*, **23**, 919 (1988).
23. U.P. Singh, Ph.D. Thesis, Magnetic and Electrical Transport Properties on Rare Earth and Transition Metal Mixed Compounds at High Temperature, V.B.S. Purvanchal University, Jaunpur (2002).
24. G.G. Robert, *Phys. Stat. Sol.*, **27**, 209 (1968).
25. R.R. Heiks and R.W. Ure, Thermoelectricity Science and Engineering, New York, Interscience, p. 45 (1961).

(Received: 24 March 2006;

Accepted: 26 February 2007)

AJC-5449